Available online at www.sciencedirect.com
ScienceDirect
Chinese Chemical Letters 21 (2010) 492–495
CHINESE CHEMICAL LETTERS
www.elsevier.com/locate/cclet

Mechanisms of imidacloprid resistance in *Nilaparvata lugens* by molecular modeling

Gen Yan Liu [a,b], Wei Miao [a], Xiu Lian Ju [a,b,*]

[a] *Key Laboratory for Green Chemical Process of Ministry of Education, School of Chemical Engineering & Pharmacy, Wuhan Institute of Technology, Wuhan 430073, China*

[b] *Key Laboratory of Pesticide Chemistry and Application, Ministry of Agriculture, The Chinese Academy of Agricultural Sciences, Beijing 100193, China*

Received 17 August 2009

Abstract

Homology models of the ligand binding domain of the wild-type and Y151S mutant brown planthopper (*Nilaparvata lugens*) α1 and rat (*Rattus norvegicus*) β2 nicotinic acetylcholine receptor (nAChR) subunits were generated based on the crystal structure of acetylcholine binding protein of *Lymnaea stagnalis*. Neonicotinoid insecticide imidacloprid was docked into the putative binding site of wild-type and mutant α1β2 dimeric receptors by Surflex-docking, and the calculated docking energies were in agreement with experimental results. The resistance mechanisms and corresponding binding modes of imidacloprid on nAChRs containing the Y151S target-site mutation were discussed.

Keywords: nAChR; Imidacloprid; Homology model; Docking; Resistance

Neonicotinoids as nicotinic acetylcholine receptor (nAChR) agonists with potent insecticidal activity are extensively used worldwide for both crop protection and animal health application. Imidacloprid (IMI), a chloropyridine-based nitroamidine compound, was the pioneer of neonicotinoids, and subsequently six additional neonicotinoids have been marketed since the introduction of IMI in 1991 [1–3]. Radioligand binding assays and electrophysiological studies have established that all neonicotinoid insecticides act on the insect central nervous system (CNS) as agonists of the postsynaptic nAChRs and have revealed that IMI has selective toxicity on insects over mammals [4]. However, since the introduction of imidacloprid, evidence of resistance has been slow to emerge but now involves a number of important insects included whitefly (*Bemisia tabaci*), brown planthopper (*Nilaparvata lugens*) and wheat aphid (*Sitobion avenae*), *etc*. [5].

Most of the insect nAChR subunits have been cloned, and genome sequencing of several insects also gives more information about insect nAChRs. For instance, five nAChR subunits (Nlαl–Nlα4 and Nlβ1) were cloned from *N. lugens* [6]. However, the functional architecture and diversity of insect nAChRs were less well understood in contrast to mammals [2,3]. To date, no reports of *in vitro* expression of a fully functional nAChR have been published for

* Corresponding author at: School of Chemical Engineering & Pharmacy, Wuhan Institute of Technology, Wuhan 430073, China.
E-mail address: xiulianju2008@yahoo.com.cn (X.L. Ju).

1001-8417/$ – see front matter
doi:10.1016/j.cclet.2009.12.017

insects and a crystal structure of the insect nAChR complexed with neonicotinoids has not yet been existed. Most information about the functionality of insect subunits has come from studies in which α-subunits were co-expressed with a vertebrate β-subunit although they may not faithfully reflect native insect nAChRs. Recently, Liu *et al*. have demonstrated that a mutation Y151S in a hybrid nAChRs containing *N. lugens* α1 and rat (*Rattus norvegicus*) β2 subunits was responsible for a substantial reduction in specific [^{3}H]imidacloprid binding [6,7].

In the present study, the *N*-terminal ligand-binding domain (LBD) of wild-type and Y151S mutant *N. lugens* α1/rat β2 hybrid nAChRs were built by the homology modeling, using the crystal structure of the AChBP of *Lymnaea stagnalis* (PDB entry: 2ZJU, 2.58 Å resolution) as a template [8]. The two representative models were optimized and validated by molecular dynamics simulation as well as by comparison with experimental results. Especially, neonicotinoid imidacloprid was docked to the binding sites of the two models, respectively, and the results were used to explain and consolidate experimental data. Meanwhile, the mechanisms of resistance to imidacloprid in *N. lugens* nAChRs were studied.

The nAChRs are members of the cys-loop superfamily of pentameric ligand-gated ion channels (LGICs), which also include ionotropic receptors for GABA, glycine receptors and serotonin type 3 receptors [9,10]. Each nAChR subunit possesses an *N*-terminal extracellular LBD with a conserved di-cysteine loop, four transmembrane regions (TM1–TM4), and a large intracellular loop between TM3 and TM4. The LBDs, which are around 210 amino acid residues long, bear ligand-binding sites for agonists and competitive antagonists. The binding sites are located at the LBD interface and formed by loops A, B and C of the α subunit and loops D, E and F which are normally located at α or non-α subunit [11–13].

All calculations were performed using the SYBYL 7.3 software package (http://www.tripos.com/) running on Linux workstation [14]. The sequences of the *N. lugens* α1 (Q6U4C0) and rat β2 (P12390) nAChR subunits were obtained from TrEMBL/Swiss-Prot database. The two sequences were all edited to remove four transmembrane regions (TM1–TM4), and an intracellular loop between TM3 and TM4. A multiple sequence alignment of Ls-AChBP with *N. lugens* α1 and rat β2 was generated by the module Align and Write MSF with default parameters. The sequences and structures were structurally aligned using ORCHESTRAR program of the BATON method [15]. Meanwhile, to obtain a mutant α1 subunit, the amino acid tyrosine 151 of *N. lugens* α1 subunit in loop B was replacement by serine using the module mutation. All target peptide chains were built by recognizing the structure conserved regions (SCR), searching the gaps and adding the side chains. To generate a dimeric assembly, the α1 and β2 subunits were superimposed onto the A-chain and B-chain of 2ZJU structure, respectively (Fig. 1). Both of the obtained dimer models were optimized energetically using AMBER7 FF99 force field by performing a conjugate gradient minimization with 10,000 step iterations to reach a root-mean-square (RMS) gradient energy of 0.5 kcal/mol Å.

Subsequently, in order to determine whether the LBD of the dimeric nAChRs was stable, molecular dynamics (MD) simulations were performed on both of the modeled receptors over 500 ps with the step size of 1 fs at a constant temperature 300 K [14]. According to dynamics simulation, the potential energy of these models declined in the

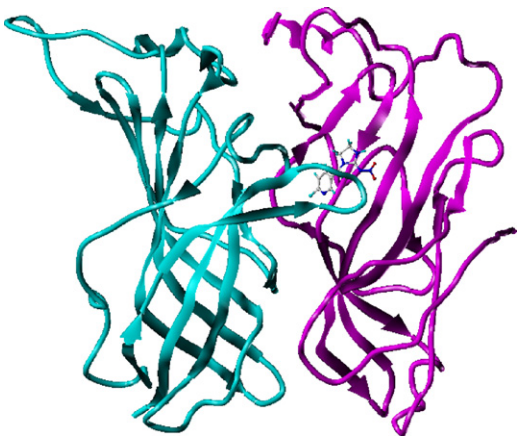

Fig. 1. A ribbon representation of the *N. lugens* α1/rat β2 dimer with imidacloprid. Cyan: α1 subunit, magenta: β2 subunit. (For interpretation of the references to color in this figure legend, the reader is referred to the web version of the article.)

Table 1
The results of docking.

Model	I_{max} (nA)[a]	EC_{50} (μmol/L)[b]	Score	Free energy of binding (kcal/mol)	H-bond
Nlα1β2	172 ± 2.3	67 ± 2.6	3.83	−5.20	Y
Nlα1^{Y151S} β2	22 ± 0.5	177 ± 3.4	2.34	−3.18	N

[a] I_{max}: maximum normalized response (from literature [7]).
[b] EC_{50}: half maximum concentration (from literature [7]).

beginning and remained stable subsequently. As a result, two representative models of wild-type and mutant *N. lugens* α1/rat β2 hybrid nAChRs have been constructed to study the resistant mechanism of imidacloprid in *N. lugens*.

The Surflex scoring function, which is based on the binding affinities of protein–ligand complexes, takes into account several terms, including hydrophobic, polar, repulsive, entropic and salvation [16]. The docking scores are expressed in $-\log_{10} K_d$ units to evaluate the docking results, where K_d represents a dissociation constant of a ligand. In present study, the binding free energies (kcal/mol) of protein–ligand complexes would be obtained according to the calculation as follows, where RT = 0.59 kcal/mol.

$$\text{Free energy of binding} = \text{RT} \ln K_d \quad (1)$$

The statistical results of docking were listed in Table 1. The calculated binding free energies of protein–ligand complexes of wild-type and mutant models were −5.20 kcal/mol and −3.18 kcal/mol, respectively. These results are in agreement with the experimental data, imidacloprid exhibited a 2.7-fold shift in EC_{50} on nAChR receptors containing the Nlα1Y151S subunit (EC_{50} = 177 μmol/L) as compared with nAChR receptors containing the wild-type subunit (EC_{50} = 67 μmol/L) [7].

The structure of the α subunit and IMI binding mode in the wild-type and the mutant models are shown in Fig. 2. The root-mean-square deviation (RMSD) of structure of α subunit in the wild-type model and the mutant model is 0.364 Å, indicating that the mutagenesis cause conformational changes. Additionally, the RMSD value of the binding sites of two models is 0.885 Å, the difference of structural conformation of the binding sites of two models is more significant. The detailed alignment of two binding sites of α subunit was shown in Fig. 2a.

In the case of the mutant nAChR binding pocket, we observed that the Trp149, Thr150 and Tyr199 shift toward the inner of the cavity. A similar shift of Trp149 in the middle of the binding site was also observed by Bisson et al. [17]. From Fig. 2a, we speculate that the shift may make the cavity formed by Trp149, Thr150 and Tyr199 narrow, which result in that the pyridine ring of IMI is difficult to entrance this pocket. And the docking results support our hypothesis.

The detailed binding mode was shown in Fig. 2b and 2c. The nitrogen atom of the pyridine ring of IMI was formed a hydrogen bond with the side chain of Tyr199 of loop C in the wild-type model, which was not observed in the mutant model. The cation–π interactions between the nitrogen atoms of imidazolidine ring with Phe118 of loop E were

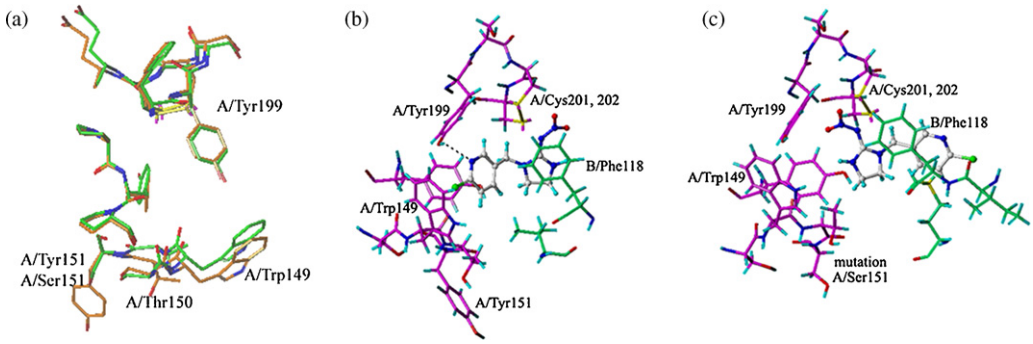

Fig. 2. IMI binding analyses based on the homology model. (a) Alignment of the binding sites of α subunit in two models (orange: the wild-type model; green: the mutant model); (b) a detailed view of the binding site and hydrogen bonds of the wild-type α1β2 model with imidacloprid; and (c) a detailed view of the binding site of the mutant α1β2 model with imidacloprid without hydrogen bonds. The detailed hydrogen bonds are displayed by black dotted line. (For interpretation of the references to color in this figure legend, the reader is referred to the web version of the article.)

observed in two complexes. Consistent with this result, Tomizawa and Casida have earlier demonstrated cation–π interactions of the tryptophan residue with the imidazolidine ring containing negatively charged nitrogens [2,3]. Specially, the chlorine atom was located in the vicinity of the indole ring of Trp149 of loop B, which made van der Waals contact the side chain of this amino acid of the wild-type model. Intriguingly, the weakly binding IMI adopt two different binding orientations at the mutant nAChR binding pocket, whereas a single tight binding conformation reflects the high affinity to the wild-type nAChR. From above analysis, the mutagenesis may cause the conformational changes of the whole α subunit to reduce the sensitivity of the binding site for IMI although the directed interactions between IMI and Tyr151 or Ser151 were not found.

In conclusion, three-dimensional models of wild-type and Y151S mutant *N. lugens* α1/rat β2 hybrid nAChRs were generated by homology modeling based on the crystal structure of the acetylcholine-binding protein (AChBP) of *L. stagnalis*. Neonicotinoids insecticide IMI was docked into the putative binding site of the wild-type and Y151S mutant *N. lugens* nAChRs by Surflex-docking, and the calculated docking energies were in agreement with the experimental results. Docking studies suggested that the conformation of the Y151S mutant subunits of *N. lugens* has changed, resulting in reduced binding affinity. These results may be of valuable guidance for resistance management of imidacloprid.

References

[1] K. Matsuda, S.D. Buckingham, D. Kleier, et al. Trends Pharmacol. Sci. 22 (2001) 573.
[2] M. Tomizawa, J.E. Casida, Annu. Rev. Entomol. 48 (2003) 339.
[3] M. Tomizawa, J.E. Casida, Annu. Rev. Pharmacol. Toxicol. 45 (2005) 247.
[4] K. Matsuda, M. Shimomura, M. Ihara, et al. Biosci. Biotechnol. Biochem. 69 (2005) 1442.
[5] R. Nauen, I. Denholm, Arch. Insect Biochem. Physiol. 58 (2005) 200.
[6] Z. Liu, M.S. Williamson, S.J. Lansdell, et al. Proc. Natl. Acad. Sci. U.S.A. 102 (2005) 8420.
[7] Z. Liu, M.S. Williamson, S.J. Lansdell, et al. J. Neurochem. 99 (2006) 1273.
[8] M. Ihara, T. Okajima, A. Yamashita, et al. Invert. Neurosci. 8 (2008) 71.
[9] M.O. Ortells, G.G. Lunt, Trends Neurosci. 18 (1995) 121.
[10] H.A. Lester, M.I. Dibas, D.S. Dahan, et al. Trends Neurosci. 27 (2004) 329.
[11] K. Brejc, W.J. van Dijk, R.V. Klaassen, et al. Nature 411 (2001) 269.
[12] J.A. Dani, Biol. Psychiatry 49 (2001) 166.
[13] J.M. Lindstrom, Ann. NY. Acad. Sci. 998 (2003) 41.
[14] SYBYL software, Version 7.3, Tripos Associates Inc, St. Louis, 2006.
[15] Z.Y. Zhu, A. Sali, T.L. Blundell, Protein Eng. 5 (1992) 43.
[16] A.N. Jain, J. Comput. Aided Mol. Des. 10 (1996) 427.
[17] W.H. Bisson, G. Westera, P.A. Schubiger, et al. J. Mol. Model 14 (2008) 891.